Seasonal biodegradation of the artificial sweetener acesulfame enhances its use as a transient wastewater tracer

Miguel Angel Marazuela [1,], Giovanni Formentin [1,2], Klaus Erlmeier [1], Thilo Hofmann [1,*]*

[1] Centre for Microbiology and Environmental Systems Science, Department of Environmental Geosciences, University of Vienna, Josef-Holaubek-Platz 2 UZAII, 1090 Vienna, Austria

[2] HPC Italia Srl, via Francesco Ferrucci 17/A, 20145 Milano, Italy

***Corresponding authors: thilo.hofmann@univie.ac.at; miguel.angel.marazuela@univie.ac.at*

Abstract

The persistence of the artificial sweetener acesulfame potassium (ACE) in wastewater treatment and subsequently in the aquatic environment has made it a widely used marker of wastewater in both surface water and groundwater. However, the recently observed biodegradation of ACE during wastewater treatment has questioned the validity of this application. In this study, we assessed the use of ACE not only as a marker of wastewater, but also as a transient wastewater tracer that allows both the calculation of mixing ratios and travel times through the aquifer as well as the calibration of transient groundwater flow and mass transport models. Our analysis was based on the data obtained in a nearly 8-year river water and groundwater sampling campaign along a confirmed wastewater-receiving riverbank filtration site located close to a drinking water supply system. We confirm that temperature controls ACE concentrations and thus their seasonal oscillation. River water data showed that ACE loads decreased from 1,500-4,000 $\mu g \cdot s^{-1}$ from December to June (cold season; T<10°C) to 0-500 $\mu g \cdot s^{-1}$ from July to November (warm season; T>10°C). This seasonal oscillation was transferred to the aquifer and preserved >3 km through the aquifer, with ACE concentrations oscillating between values below the detection limit in the warm

season to 0.15 $\mu g \cdot L^{-1}$ in the cold season. The seasonal variation in ACE degradation during wastewater treatment enables the sweetener's use as a transient tracer of wastewater inflows and riverbank filtration. In addition, the arrival time of the ACE concentration peak can be used to estimate groundwater flow velocity and mixing ratios, thereby demonstrating its potential in the calibration of groundwater numerical models.

Keywords: environmental tracer; wastewater treatment; riverbank filtration; groundwater model; groundwater age; emerging contaminant.

1. Introduction

Environmental tracers are natural or anthropogenic substances that, while present in concentrations that do not pose a risk to human health, can still be measured in surface water and in groundwater. They have thus been exploited in assessments of the source, trajectory, and mixing dynamics of wastewater released into the environment (Massmann et al., 2008; McCance et al., 2018; Stoewer et al., 2015; Turnadge and Smerdon, 2014). The most useful environmental tracers are hardly degradable by biochemical processes during wastewater treatment or subsequently in the aquifer, are widespread in the environment, and their concentrations fluctuate over time.

The potassium salt of acesulfame (ACE) is 200× sweeter than sugar, which together with its stability (Li et al., 2021; Lino et al., 2008) accounts for it being the most widely used sugar substitute, whether in food, cosmetics, or medicines. The accepted daily intake of ACE is 15 $mg \cdot kg^{-1}$ of body weight (USFDA, JECFA). However, since ACE cannot be metabolized in the human body after ingestion, it is excreted unchanged through the renal system (Renwick, 1986). Consequently, most of the consumed ACE finally ends up in wastewater treatment plants (WWTPs), from where it is discharged into the environment (Volz et al., 1991). As ACE is highly hydrophilic, following its release from WWTPs into streams it spreads easily through the aquatic environment and is therefore frequently detected in surface water, groundwater, and even drinking water (Buerge et al., 2009; Gan et al., 2013; Scheurer et al., 2011, 2009). ACE has been globally measured in wastewater effluents, with concentrations ranging from below the limit of quantification (LOQ) to 2500 $\mu g \cdot L^{-1}$ (e.g., Arbeláez et al., 2015; Belton et al., 2020; Buerge et al., 2009; Gan et al., 2013; Kokotou and Thomaidis, 2013; Lee et al., 2015; Loos et al., 2013; Ordóñez et al., 2012; Sanz-Prat et al.,

2020; Scheurer et al., 2009; Van Stempvoort et al., 2020). Average ACE concentrations of 2.9 $\mu g \cdot L^{-1}$ (<LOQ to 53.7 $\mu g \cdot L^{-1}$) in surface water and 0.653 $\mu g \cdot L^{-1}$ (<LOQ to 9.7 $\mu g \cdot L^{-1}$) in groundwater have been reported in Europe, America, and Asia (Belton et al., 2020). Although the adverse effects of sweeteners at the high concentrations used in foodstuffs (taste threshold of 8.94 mg L^{-1}) continue to be debated, the concentrations found in surface, groundwater, or drinking water are considered to be below those exerting toxic effects (Belton et al., 2020; Dietrich et al., 2021).

The persistence of ACE after human ingestion and municipal wastewater treatment (Buerge et al., 2009; Gan et al., 2013; Jekel et al., 2015; Oppenheimer et al., 2011; Scheurer et al., 2009; Soh et al., 2011; Subedi and Kannan, 2014; Tran et al., 2015) makes it an excellent tracer of: wastewater input into environmental waters (Ishii et al., 2021; Lange et al., 2012; Scheurer et al., 2011, 2009; Sérodes et al., 2021; Van Stempvoort et al., 2013, 2011b), septic wastewater plume migration in aquifers (Robertson et al., 2013; Snider et al., 2017; Spoelstra et al., 2020; Van Stempvoort et al., 2011a; Wolf et al., 2012), and riverbank filtration (Datel and Hrabankova, 2020; Engelhardt et al., 2014a, 2014b, 2013; Roy and Bickerton, 2010; Sanz-Prat et al., 2020). In fact, ACE meets most of the requirements of an ideal wastewater tracer (Dickenson et al., 2011; Gasser et al., 2010; Oppenheimer et al., 2011) as: i) it is found in most wastewater sources globally, ii) it is present in wastewater at concentrations well above the LOQ (≈0.01 $\mu g \cdot L^{-1}$) (Buerge et al., 2009), iii) once in the aquifer, it travels in the dissolved phase at the average groundwater velocity, with no losses by chemical or biological attenuation processes (Datel and Hrabankova, 2020; Hwang et al., 2019; Roy and Bickerton, 2010), iv) it is either absent or it is present at concentrations orders of magnitude lower in natural groundwater, given its anthropogenic origin, and v) it can be

94 easily analyzed with affordable techniques, minimal matrix interference, and good accuracy
95 and precision.

96 However, despite the utility of ACE as a wastewater marker in rivers, lakes, and aquifers,
97 reports of its biodegradation during municipal wastewater treatment and via biotic processes
98 have questioned its value as an environmental tracer (e.g., Castronovo et al., 2017; Huang et
99 al., 2021; Hwang et al., 2019; Kahl et al., 2018; Van Stempvoort et al., 2020), which has
100 mostly included its use in calculations of groundwater residence times, the calibration of
101 transient hydrogeological models, and the differentiation of multiple sources of
102 contamination (Engelhardt et al., 2014a, 2013; Gerber et al., 2018; Purtschert, 2008; Van
103 Stempvoort et al., 2013). Buerge et al. (2011) reported the dissipation of at least 60% of ACE
104 during aerobic incubation over 70 days while Burke et al. (2014), using material from the
105 oxic to suboxic zone of a riverbank filtration site in a laboratory column experiment, reported
106 ACE attenuation of almost 50% and the temperature dependence of the reaction, as ACE was
107 eliminated at 20°C but not at 6.5°C. The biodegradation of ACE by nitrifying activated
108 sludge reached 21% after 7 days (Tran et al., 2014). Castronovo et al. (2017) reported ACE
109 biodegradation in German and Swiss WWTPs under aerobic and anaerobic conditions and
110 the transformation of ACE into sulfamic acid. Recently, a lab-scale study demonstrated that
111 ACE can be catabolized completely by an enrichment culture in which it is the sole carbon
112 source (Kahl et al., 2018), while other studies have shown the involvement of different
113 bacterial strains in ACE degradation (Huang et al., 2021; Kleinsteuber et al., 2019).

114 Furthermore, after studying nine German WWTPs, Kahl et al. (2018) concluded that
115 ACE removal efficiency is highly variable during the year, with a clear seasonal pattern,
116 especially in small to medium WWTPs, where the temperature-driven removal of ACE plays

117 an important role. Monthly median removal exceeded 95% from July to October/November,
118 with < 15% of the ACE removed between January and April. Literature data suggest that the
119 degradation of ACE in WWTPs first occurred in 2010, with a greater capability in small to
120 medium plants without oxygen and temperature impediments. Li et al. (2020) reported
121 removal rates of 74 ± 42% in a study carried out in 69 WWTPs across Australia. Despite this
122 seasonal removal, after analyzing 12 WWTPs and 7 septic systems, Van Stempvoort et al.
123 (2020) demonstrated that the residual concentrations of ACE in effluents and septic plumes
124 are still sufficient to allow the use of ACE as a tracer for identifying the presence or absence
125 of wastewater in groundwater.

126 Environmental tracers whose concentrations exhibit large oscillations in their amplitude
127 and duration have a broad range of applications (Herrera et al., 2022b, 2022a; Massoudieh,
128 2013; Thiros et al., 2021). As daily or weekly oscillations of a tracer are damped after a few
129 meters of traveling through an aquifer (Brünjes et al., 2016), tracers with seasonal oscillations
130 are more suitable for large-scale tracing (Molina-Giraldo et al., 2011). However, the
131 suitability of ACE as a transient environmental tracer has yet to be determined. Thus, in this
132 study we assess the use of ACE as a transient tracer of wastewater after its seasonally varied
133 biodegradation during municipal wastewater treatment. Our results show that, as a transient
134 tracer, ACE has several important applications, including in calculations of groundwater
135 travel times and mixing ratios, the identification of wastewater sources, especially in urban
136 environments, and in reducing the uncertainties in groundwater flow and mass transport
137 models. Moreover, its use can improve investigations of riverbank filtration systems that can
138 affect water quality in drinking water supply systems.

2. Materials and methods

A river water and groundwater ACE sampling campaign of nearly 8 years duration was carried out along a confirmed wastewater-affected riverbank filtration site. In addition, the transport of ACE through the aquifer was simulated in a groundwater flow and ACE transport model, described below.

2.1. Study area

The investigation area is located in a pre-alpine catchment in Europe, covering an area of 5 km^2. It was extensively described in previous studies (Bichler et al., 2016, 2014; Brünjes et al., 2016; Stoewer et al., 2015) (Fig. 1). In brief, the site is characterized by a temperate climate with a long-term annual mean precipitation of 1,300 mm and a mean air temperature of 8.9°C. Groundwater recharge, estimated according to the FAO guideline, is between 25% and 65% of total rainfall (Allen et al., 1998).

FIGURE 1

The study area is composed of two fluvio-glacial aquifers, Aquifer 1 and Aquifer 2, converging at the confluence of the respective rivers (Rivers 1 and 2), and whose basements consist of impermeable tertiary rocks (Fig. 1). The aquifers are largely unconfined or semiconfined and are composed of a heterogeneous matrix of gravel, sand, and clay. The thickness of the quaternary sediments ranges from a few meters to 70 m, with an average saturated thickness of 15 m and a maximum of 30 m (see vertical profiles in Fig. 1). Hydraulic conductivities are estimated to be in the range of 10–5,000 $m \cdot d^{-1}$, based on pumping tests and estimations from other, analogous sites (Theel et al., 2020). Water column pressure is continuously measured at 31 wells using data loggers.

The mean discharge of River 1, recorded at a gauging station located approximately 3 km upstream of the investigation area, is 8.5 $m^3 \cdot s^{-1}$; the flood discharge, with a return period of one year, is 38 $m^3 \cdot s^{-1}$. Part of the discharge of River 1 is diverted upstream of the investigation area, leading to a constant discharge into the latter of 1.2 $m^3 \cdot s^{-1}$. The average discharge of River 2 is 1.3 $m^3 \cdot s^{-1}$. In addition, 4 km upstream of the study area, River 1 receives the effluent of a WWTP at an average rate of 0.11 $m^3 \cdot s^{-1}$ (Brünjes et al., 2016). The WWTP serves a population of 27,000 inhabitants. The wastewater contribution to River 1 leads to a wastewater load of 1.3% of the volumetric flow rate during average flow conditions. The level of River 1 is always above the water table, which favors riverbank filtration from stretches identified in previous studies (Bichler et al., 2016) and highlighted in red in Fig. 1. The infiltration rate is in the range of 100–400 $L \cdot s^{-1}$, calculated based on the difference between the river discharge measured above and below the release site.

Close to the confluence of Rivers 1 and 2 and 3,250 m downstream of the riverbank filtration, a drinking water supply system extracts an average of 1,500 $L \cdot s^{-1}$. The waterwork operates a horizontal drain that uses gravity to remove groundwater from the aquifer and then drive the water to the collector well. The last 130 m of the horizontal drain are sealed.

Three different water types at the investigation area were identified in an earlier study (Bichler et al., 2016): regional recharge harder groundwater (RGW), bank-filtration-influenced softer groundwater (BF), and groundwater with a higher NaCl content. All three types belong to the calcium–magnesium–bicarbonate water type that is typical of waters in limestone-dominated catchments (Appelo and Postma, 2005; Hoehn and Scholtis, 2011). The RGW type, characterized by high levels of mineralization (TDS: 577 $mg \cdot L^{-1}$) and a high chloride concentration (9.8 ± 1.8 $mg \cdot L^{-1}$), is not affected by riverbank filtration. BF water is

a mixture of RGW and riverbank filtrate and is characterized by less mineralization (TDS: 359.4 $mg \cdot L^{-1}$) and a lower chloride concentration (7.5 ± 1.4 $mg \cdot L^{-1}$). Based on mixing ratios of chloride and gadolinium, the fraction of riverbank filtrate was estimated to be 76–100% in the infiltration area and 37–67% near the waterwork (Bichler et al., 2016). ACE concentrations range from below the LOQ up to 0.5 $\mu g \cdot L^{-1}$. Water samples with a higher NaCl concentration (NaCl type) are restricted to Aquifer 2.

2.2. Sample collection

River water was collected as grab samples weekly from May 1, 2020 to December 17, 2021 at three points (R1.1, R1.2, and R1.3 in Fig. 1). Since the anthropogenic origin of ACE and its persistence in municipal treated wastewater were demonstrated by Bichler et al. (2016), long-term sampling was not considered for the WWTP influent/effluent.

Groundwater ACE concentrations were assessed every 2 weeks from March 10, 2014 to December 15, 2021. The horizontal drain (D1) was sampled at its start and end points (D1-A and D1-B, respectively). D1-A was reached using a vertical pipe equipped with a tap, and D1-B directly from the collector well.

2.3. Laboratory analyses

ACE was analyzed following the method described by Scheurer et al. (2009). In short, samples prepared using solid-phase extraction were analyzed using liquid chromatography on an HPLC system (1200 SL; Agilent Technologies, Japan) connected to an API 4000 Q-trap triple-quadrupole mass spectrometer (Applied Biosystems/MDS Sciex Instruments, USA) operated in negative electrospray ionization mode. The LOQ was 0.02 $\mu g \cdot L^{-1}$, with a standard deviation of 0.004 $\mu g \cdot L^{-1}$.

206 *2.4. Numerical model*

207 A two-dimensional (2D) model encompassing the investigation area was established to
208 simulate groundwater flow and ACE transport from River 1 to the drinking water supply
209 system. The numerical model was set up in the finite-element code FEFLOW®, which allows
210 the solving of equations describing groundwater flow and mass transport under saturated
211 conditions (Diersch, 2014). A summary of the main features of the model and its parameters
212 is provided in Table SI-1. The FEFLOW® internal grid-builder routine was applied to
213 generate a numerical mesh consisting of 15,512 triangular elements and 7,944 nodes. The
214 simulation covered the period September 1, 2020 to December 31, 2021, with an automatic
215 time step control scheme and a maximum time step of 1 day. The simulation period was
216 selected to allow the reproduction of ACE propagation through the aquifer for more than one
217 complete seasonal biodegradation cycle. Initial conditions for all hydraulic and transport
218 variables were calculated in a previous steady-state simulation representing the mean
219 hydrogeological functioning of the system for the last decade (2012–2021). An initial spin-
220 up period of 2 months was considered sufficient for the simulation results to become
221 independent of the initial conditions.

222 Groundwater inflow through the upstream boundaries of Aquifers 1 and 2 was simulated
223 using a Cauchy-type boundary condition (BC) with a reference hydraulic head time series
224 based on the levels measured in neighboring wells. An ACE concentration of 0 $\mu g \cdot L^{-1}$ was
225 set at these boundaries. The downstream boundary was a Cauchy-type condition with a
226 reference hydraulic head based on the levels measured at the closest monitoring well. A free-
227 mass outflow BC was applied to this downstream boundary. Recharge by precipitation was
228 set on the model based on data registered at the local weather station and considering the

local infiltration rate. The ACE concentration in the recharge from precipitation was set to 0 $\mu g \cdot L^{-1}$. Riverbank filtration was reproduced through a Well-type BC for water flow and a Cauchy-type BC for ACE mass based on the transient seasonal ACE concentration measured in river water. No-flow and no-mass-flow conditions were applied to all remaining boundaries. The horizontal drain collecting groundwater was represented by discrete 1D elements with high hydraulic conductivity. At the end of the screened stretch of the drain, a Well-BC was operational, with the extraction flow measured using a flow meter.

The model was automatically calibrated against the hydraulic heads and ACE concentrations using FEPEST®, which is the FEFLOW®-integrated version of the model-independent parameter estimation code PEST (Doherty, 2015). Transmissivity, specific storage, and porosity were calibrated considering 183 pilot points for each of these parameters. Tikhonov, Singular Value Decomposition, and SVD-Assist were chosen for regularization by prior information, subspace, and super parameters, respectively. Initial and preferred values of transmissivity were chosen by taking into account pumping test information and the real saturated thickness in each zone of the aquifer. Transfer rates associated with Cauchy-type BCs and the longitudinal and transverse dispersivities (linking the two parameters by a ratio of 10:1) were also calibrated. A Python plugin developed with the integrated Interface Manager (IFM) enabled the calibration of Well-type BCs and the subsequent estimation of the infiltration rate from the riverbank filtration source.

3. Results and discussion

3.1. Seasonal oscillations of ACE allows its use as transient tracer

ACE concentrations showed a clear temperature-linked seasonal oscillation pattern, with maximum concentrations in the range of 0.2–1 $\mu g \cdot L^{-1}$ occurring between December and June (cold season; T<10°C) and minimum concentrations of 0–0.1 $\mu g \cdot L^{-1}$ between July and November (warm season; T>10°C) (Fig. 2A and Table SI-2). Due to the small catchment area, the ACE concentrations were within the lower range of those reported for rivers worldwide (Belton et al., 2020). Seasonal oscillation was confirmed by calculating the total load in River 1, eliminating dilution by discharge; ACE loads were 1.5–4 $mg \cdot s^{-1}$ during the cold season, which was still around one order of magnitude above the loads of 0–0.5 $mg \cdot s^{-1}$ measured during the warm season (Fig. 2B and Table SI-2). Therefore, dilution by changes in river discharge can be ruled out as the process explaining the seasonal oscillation of ACE concentrations. Also, previous studies showed that ACE consumption throughout the year is fairly stable or even slightly higher in summer, when the demand for sweetened foodstuffs, especially beverages and ice cream, increases (Lange et al., 2012; Li et al., 2021), which would lead to a seasonal pattern opposite to that observed. In addition, the calculated daily per capita ACE load of 0.8 ± 0.8 mg resulting from the warm season (calculated considering 27,000 inhabitants) was more than one order of magnitude lower than the daily per capita loads reported for other central European countries (e.g., Switzerland: 5.7–17.6 mg, Germany: 5.8–12.7 mg, Austria: 4.9 mg; Lange et al., 2012), which indicated that an additional process is responsible for ACE removal during the warm season. This was supported by also calculating the daily per capita ACE load during the cold season, which was 8.8 ± 3 mg, an amount closely aligned with the loads reported for other central European countries.

FIGURE 2

The recently discovery of a temperature-dependent seasonal biodegradation of ACE during wastewater treatment (Kahl et al., 2018) is the most straightforward explanation for the observed seasonal oscillations in the ACE concentration and the almost perfect correlation between ACE loads (Fig. 2B) and water/air temperature (Fig. 2C). Minimum air and river-water temperatures were reached in January 2021 (T≈0°C), after a sharp temperature drop beginning in August 2020 and preceding a gradual temperature rise until June 2021. The same asymmetric trend characterized ACE loads, although with a delay of a roughly two months, probably due to the time required by bacteria to equilibrate to the new temperature (compare Fig 2B and C). In addition, the ACE concentration changed rapidly, reflecting the sudden rise in the load in January and the sharp decrease in June. Although degradation rate calculations were not within the scope of this study, the measured ACE concentrations and loads were in accordance with the rates estimated by Kahl et al. (2018) for other WWTPs in Germany, i.e., close to 0% during the cold period and close to 100% during the warm period.

Although this seasonal oscillation may be less prominent in wastewaters from large WWTPs, in which both the temperature and available oxygen are controlled (Kahl et al., 2018), this pattern can probably be globally extrapolated to most surface waters receiving wastewater contributions from small and medium WWTPs, especially because the ACE concentration in the study area was lower than that measured in other rivers globally. The effect of dilution by discharge or any hypothetical oscillation in ACE consumption over the year would be limited to short periods, such as the peak that occurred in January 2021, which was mainly explained by a significant reduction in river discharge during that month (Fig. 2A). An increase in ACE consumption during the Christmas holidays could also help to

296 explain the slight asymmetry in the seasonal oscillation of the ACE load, with a maximum
297 occurring in January rather than in the middle of the cold season (Fig. 2B).

298 *3.2. ACE seasonal oscillation propagates from surface- to groundwater*

299 The ACE concentrations measured in groundwater, at D1-A and D1-B (Fig. 1),
300 demonstrated the transfer and persistence of the seasonal oscillation of ACE into and through
301 the aquifer (Fig. 3 and Table SI-2). The ACE concentration in groundwater sampled at the
302 drinking water supply system oscillated between 0 $\mu g \cdot L^{-1}$ in the warm season and up to 0.15
303 $\mu g \cdot L^{-1}$ in the cold season. This seasonal change was propagated by the river water that
304 infiltrated 3,250 m upstream of the drinking water supply system, indicating a fairly
305 conservative behavior through the aquifer and demonstrating that the ACE seasonal
306 oscillation can be tracked at distances of several kilometers.

307 FIGURE 3

308 The similarity of the ACE concentrations measured at D1-A and D1-B was consistent
309 with a preferential flow from D1-A to D1-B along the horizontal drain (see Fig. 1). The small
310 reduction in the ACE concentration from D1-A to D1-B can be explained by contributions
311 of external water to the drain along this stretch, which is screened along most of its length.
312 The ACE peak in groundwater was detected in most years in March, around 2 months after
313 the detection in river water (Fig. 3). This finding is analyzed in detail in the following section.

314 *3.3. ACE can be used to elucidate riverbank filtration and to calibrate numerical*
315 *groundwater flow and transport models*

316 The numerical model reproduced the propagation of the seasonal oscillation in the ACE
317 concentration for more than one year. The simulated riverbank filtrate propagated along the

central-eastern part of Aquifer 1 from the riverbank filtration source to the drinking water supply system (Fig. 4). The groundwater ACE concentration close to the infiltration area ranged between <LOQ in the warm session and 0.79 $\mu g \cdot L^{-1}$ in the cold season. The similar concentrations in river water and groundwater indicated a very good hydraulic connection at that stretch of the river. The model estimated an infiltration rate of 369 $L \cdot s^{-1}$, consistent with the measured differential discharge up- and downstream of the riverbank filtration stretch. At both sampling points of the drinking water supply system, D1-A and D1-B, the ACE concentration ranged from a minimum close to the LOQ in the warm season to a maximum of almost 0.15 $\mu g \cdot L^{-1}$ in the cold season (Fig. 5). The alignment of the ACE concentrations at the two sampling points indicated the fast flow along the drain. Riverbank filtration mixing ratios > 80% were calculated in the area closest to the infiltration source (Fig. 6), consistent with the mixing ratios of 76–100% estimated by Bichler et al. (2016) based on chloride and gadolinium. The mixing ratios were reduced to 27% and 22% at D1-A and D1-B, respectively. The good fit of the non-reactive model to the observed ACE concentrations and the apparent persistence of the seasonal oscillation 3 km downstream of the riverbank filtration source highlight the largely conservative behavior of ACE in the aquifer. The attenuation of the ACE concentration from river to groundwater observation points can be explained by dilution (e.g., Liu et al., 2014).

FIGURE 4

FIGURE 5

FIGURE 6

Despite the good connection between D1-A and D1-B, mixture along the open drain resulted in a delay of 3 days in the arrival of the ACE concentration peak from D1-A to D1-B. Specifically, the average travel time of ACE from the riverbank filtration source to the

drinking water supply system was 64 days at D1-A and 67 days at D1-B (Figs. 5B), based on the peak concentration, with a range between 40 and 90 days.

The transient behavior of ACE allows its use not only as a wastewater marker but also as a transient tracer in the identification of riverbank filtration sources and in the calculation of travel times and mixing ratios through the aquifer. A decrease in the river discharge for a period of more than one month, such as observed for River 1 in January 2021, will also contribute to an oscillation of the ACE concentration, but only if the decrease occurs during the cold season, when the ACE concentration is high.

4. Use of ACE as an oscillating wastewater marker

Chemical pollution of the aqueous environment, including inputs of xenobiotics, is ubiquitous. However, environmental scientists, albeit with good reason, have largely focused on the adverse effects of the constantly increasing number of trace pollutants to humans and the environment. Yet, in hydrogeology, groundwater contaminants, beginning with tritium, released via surface nuclear weapons testing, can serve as markers that can be exploited by hydrogeologists to better monitor and manage drinking water resources.

In this study, the temperature-dependent transient signal of ACE was investigated with respect to its properties as a wastewater marker. With concentrations far below any relevance to human health, the seasonal oscillation in the ACE concentration was used to optimize a numerical groundwater-flow model of a riverbank filtration site affected by wastewater inputs, thus allowing both a prediction of the flow path direction and calculations of the mixing ratios and travel times.

The sharp contrast in ACE loads caused by temperature-dependent biodegradation in wastewater treatment was evidenced by loads ranging from 1,500–4,000 $\mu g \cdot s^{-1}$ in the cold

season (December-June; T<10°C) to <LOQ–500 $\mu g \cdot s^{-1}$ in the warm season (July–November; T>10°C). This variation demonstrated the importance of carefully planned ACE sampling campaigns; ACE sampling conducted only during the warm season might completely miss ACE inputs whereas sampling only during the cold season could lead to an overestimation of annual ACE fluxes. The data presented herein show that a minimum of one year of sampling is needed to understand seasonal patterns of wastewater-borne ACE inputs into rivers and the influence of riverbank filtration on aquifers.

Despite the strong temperature dependence of the ACE concentration in river water, ACE behavior in the aquifer was conservative. Although ACE concentrations in the study area were in the lower range of those described globally, the seasonal oscillation could still be transferred from the river to the aquifer and preserved over transport distances > 3 km. This conservative behavior of ACE in the aquifer supports its use in large-scale wastewater tracking. The seasonal oscillation in ACE was useful to calculate river water-groundwater mixing ratios and travel times of > 2 months. ACE may allow to assess even longer travel times depending on the groundwater temperature, chemistry, and flow patterns.

In summary, the use of ACE as tracer may facilitate investigations of wastewater contamination in urban areas and riverbank filtration systems. Moreover as a transient wastewater tracer, ACE offers new approaches to better calculate groundwater travel times, calibrate numerical models, and identify wastewater infiltration points and mixing ratios.

Acknowledgments:

The authors acknowledge DHI for sponsoring the FEFLOW license.

References

Allen, R.G., Pereira, L.S., Raes, D., Smith, M., 1998. Crop Evapotranspiration (Guidelines for Computing Crop Water Requirements). Rome, Italy.

Appelo, C.A.J., Postma, D., 2005. Geochemistry, Groundwater and Pollution, 2nd Editio. ed. CRC Press, London, UK. https://doi.org/Appelo, C.A.J., & Postma, D. (2005). Geochemistry, Groundwater and Pollution (C.A.J. Appelo, & D. Postma, Eds.) (2nd ed.). CRC Press. https://doi.org/10.1201/9781439833544

Arbeláez, P., Borrull, F., Pocurull, E., Marcé, R.M., 2015. Determination of high-intensity sweeteners in river water and wastewater by solid-phase extraction and liquid chromatography-tandem mass spectrometry. J. Chromatogr. A 1393, 106–114. https://doi.org/10.1016/j.chroma.2015.03.035

Belton, K., Schaefer, E., Guiney, P.D., 2020. A Review of the Environmental Fate and Effects of Acesulfame-Potassium. Integr. Environ. Assess. Manag. 16, 421–437. https://doi.org/10.1002/ieam.4248

Bichler, A., Muellegger, C., Brünjes, R., Hofmann, T., 2016. Quantification of river water infiltration in shallow aquifers using acesulfame and anthropogenic gadolinium. Hydrol. Process. 30, 1742–1756. https://doi.org/https://doi.org/10.1002/hyp.10735

Bichler, A., Neumaier, A., Hofmann, T., 2014. A tree-based statistical classification algorithm (CHAID) for identifying variables responsible for the occurrence of faecal indicator bacteria during waterworks operations. J. Hydrol. 519, 909–917. https://doi.org/10.1016/j.jhydrol.2014.08.013

Brünjes, R., Bichler, A., Hoehn, P., Lange, F.T., Brauch, H.-J., Hofmann, T., 2016. Anthropogenic gadolinium as a transient tracer for investigating river bank filtration. Sci. Total Environ. 571, 1432–1440. https://doi.org/10.1016/j.scitotenv.2016.06.105

Buerge, I.J., Buser, H.R., Kahle, M., Müller, M.D., Poiger, T., 2009. Ubiquitous occurrence of the artificial sweetener acesulfame in the aquatic environment: An ideal chemical marker of domestic wastewater in groundwater. Environ. Sci. Technol. 43, 4381–4385. https://doi.org/10.1021/es900126x

Buerge, I.J., Keller, M., Buser, H.R., Müller, M.D., Poiger, T., 2011. Saccharin and other artificial sweeteners in soils: Estimated inputs from agriculture and households, degradation, and leaching to groundwater. Environ. Sci. Technol. 45, 615–621. https://doi.org/10.1021/es1031272

Burke, V., Greskowiak, J., Asmuß, T., Bremermann, R., Taute, T., Massmann, G., 2014. Temperature dependent redox zonation and attenuation of wastewater-derived organic micropollutants in the hyporheic zone. Sci. Total Environ. 482–483, 53–61. https://doi.org/10.1016/j.scitotenv.2014.02.098

Castronovo, S., Wick, A., Scheurer, M., Nödler, K., Schulz, M., Ternes, T.A., 2017. Biodegradation of the artificial sweetener acesulfame in biological wastewater treatment and sandfilters. Water Res. 110, 342–353. https://doi.org/10.1016/j.watres.2016.11.041

Datel, J. V., Hrabankova, A., 2020. Pharmaceuticals load in the Svihov water reservoir (Czech Republic) and impacts on quality of treated drinking water. Water (Switzerland) 12. https://doi.org/10.3390/W12051387

Dickenson, E.R.V., Snyder, S.A., Sedlak, D.L., Drewes, J.E., 2011. Indicator compounds for assessment of wastewater effluent contributions to flow and water quality. Water Res. 45, 1199–1212. https://doi.org/10.1016/j.watres.2010.11.012

Diersch, H.-J.G., 2014. FEFLOW: Finite Element Modeling of Flow, Mass and Heat Transport in Porous and Fractured Media. Springer-Verlag Berlin Heidelberg. https://doi.org/10.1007/978-3-642-38739-5

Dietrich, A.M., Pang, Z., Zheng, H., Ma, X., 2021. Mini review: Will artificial sweeteners discharged to the aqueous environment unintentionally "sweeten" the taste of tap water? Chem. Eng. J. Adv. 6, 100100. https://doi.org/10.1016/j.ceja.2021.100100

Doherty, J., 2015. Calibration and Uncertainty Analysis for Complex Environmental Models. Watermark Numerical Computing, Brisbarne, Australia.

Engelhardt, I., Barth, J.A.C., Bol, R., Schulz, M., Ternes, A., Schüth, C., van Geldern, R., 2014a. Quantification of long-term wastewater fluxes at the surface water/groundwater-interface: An integrative model perspective using stable isotopes and acesulfame. Sci. Total Environ. 466–467, 16–25. https://doi.org/10.1016/j.scitotenv.2013.06.092

Engelhardt, I., Prommer, H., Moore, C., Schulz, M., Schüth, C., Ternes, T.A., 2013. Suitability of temperature, hydraulic heads, and acesulfame to quantify wastewater-related fluxes in the hyporheic and riparian zone. Water Resour. Res. 49, 426–440. https://doi.org/10.1029/2012WR012604

Engelhardt, I., Prommer, H., Schulz, M., Vanderborght, J., Schüth, C., Ternes, T.A., 2014b. Reactive transport of iomeprol during stream-groundwater interactions. Environ. Sci. Technol. 48, 199–207. https://doi.org/10.1021/es403194r

Gan, Z., Sun, H., Feng, B., Wang, R., Zhang, Y., 2013. Occurrence of seven artificial sweeteners in the aquatic environment and precipitation of Tianjin, China. Water Res. 47, 4928–4937. https://doi.org/10.1016/j.watres.2013.05.038

Gasser, G., Rona, M., Voloshenko, A., Shelkov, R., Tal, N., Pankratov, I., Elhanany, S., Lev, O., 2010. Quantitative evaluation of tracers for quantification of wastewater contamination of potable water sources. Environ. Sci. Technol. 44, 3919–3925. https://doi.org/10.1021/es100604c

Gerber, C., Purtschert, R., Hunkeler, D., Hug, R., Sültenfuss, J., 2018. Using environmental tracers to determine the relative importance of travel times in the unsaturated and saturated zones for the delay of nitrate reduction measures. J. Hydrol. 561, 250–266. https://doi.org/10.1016/j.jhydrol.2018.03.043

Herrera, P.A., Marazuela, M.A., Formentin, G., Hofmann, T., 2022a. Towards an effective application of parameter estimation and uncertainty analysis to mathematical groundwater models. SN Appl. Sci. 4, 213. https://doi.org/10.1007/s42452-022-05086-w

Herrera, P.A., Marazuela, M.A., Hofmann, T., 2022b. Parameter estimation and uncertainty analysis in hydrological modeling. WIREs Water 9, e1569. https://doi.org/10.1002/wat2.1569

Hoehn, E., Scholtis, A., 2011. Exchange between a river and groundwater, assessed with hydrochemical data. Hydrol. Earth Syst. Sci. 15, 983–988. https://doi.org/10.5194/hess-15-983-2011

Huang, Y., Deng, Y., Law, J.C.F., Yang, Y., Ding, J., Leung, K.S.Y., Zhang, T., 2021. Acesulfame aerobic biodegradation by enriched consortia and Chelatococcus spp.: Kinetics, transformation products, and genomic characterization. Water Res. 202, 117454. https://doi.org/10.1016/j.watres.2021.117454

Hwang, H.T., Frey, S.K., Park, Y.J., Pintar, K.D.M., Lapen, D.R., Thomas, J.L., Spoelstra, J., Schiff, S.L., Brown, S.J., Sudicky, E.A., 2019. Estimating cumulative wastewater treatment plant discharge influences on acesulfame and Escherichia coli in a highly impacted watershed with a fully-integrated modelling approach. Water Res. 157, 647–662. https://doi.org/10.1016/j.watres.2019.03.041

Ishii, E., Watanabe, Y., Agusa, T., Hosono, T., Nakata, H., 2021. Acesulfame as a suitable sewer tracer on groundwater pollution: A case study before and after the 2016 Mw 7.0 Kumamoto earthquakes. Sci. Total Environ. 754, 142409. https://doi.org/10.1016/j.scitotenv.2020.142409

Jekel, M., Dott, W., Bergmann, A., Dünnbier, U., Gnirß, R., Haist-Gulde, B., Hamscher, G., Letzel, M., Licha, T., Lyko, S., Miehe, U., Sacher, F., Scheurer, M., Schmidt, C.K., Reemtsma, T., Ruhl, A.S., 2015. Selection of organic process and source indicator substances for the anthropogenically influenced water cycle. Chemosphere 125, 155–167. https://doi.org/10.1016/j.chemosphere.2014.12.025

Kahl, S., Kleinsteuber, S., Nivala, J., Van Afferden, M., Reemtsma, T., 2018. Emerging Biodegradation of the Previously Persistent Artificial Sweetener Acesulfame in Biological Wastewater Treatment. Environ. Sci. Technol. 52, 2717–2725. https://doi.org/10.1021/acs.est.7b05619

Kleinsteuber, S., Rohwerder, T., Lohse, U., Seiwert, B., Reemtsma, T., 2019. Sated by a Zero-Calorie Sweetener: Wastewater Bacteria Can Feed on Acesulfame. Front. Microbiol. 10, 1–7. https://doi.org/10.3389/fmicb.2019.02606

Kokotou, M.G., Thomaidis, N.S., 2013. Determination of eight artificial sweeteners in wastewater by hydrophilic interaction liquid chromatography-tandem mass spectrometry. Anal. Methods 5, 3825–3833. https://doi.org/10.1039/c3ay40599k

Lange, F.T., Scheurer, M., Brauch, H.J., 2012. Artificial sweeteners-A recently recognized class of emerging environmental contaminants: A review. Anal. Bioanal. Chem. 403, 2503–2518. https://doi.org/10.1007/s00216-012-5892-z

Lee, D.G., Roehrdanz, P.R., Feraud, M., Ervin, J., Anumol, T., Jia, A., Park, M., Tamez, C., Morelius, E.W., Gardea-Torresdey, J.L., Izbicki, J., Means, J.C., Snyder, S.A., Holden, P.A., 2015. Wastewater compounds in urban shallow groundwater wells correspond to exfiltration probabilities of nearby sewers. Water Res. 85, 467–475. https://doi.org/10.1016/j.watres.2015.08.048

Li, D., O'Brien, J.W., Tscharke, B.J., Choi, P.M., Ahmed, F., Thompson, J., Mueller, J.F., Sun, H., Thomas, K. V., 2021. Trends in artificial sweetener consumption: A 7-year wastewater-based epidemiology study in Queensland, Australia. Sci. Total Environ. 754, 142438. https://doi.org/10.1016/j.scitotenv.2020.142438

Li, D., O'Brien, J.W., Tscharke, B.J., Choi, P.M., Zheng, Q., Ahmed, F., Thompson, J., Li, J., Mueller, J.F., Sun, H., Thomas, K. V., 2020. National wastewater reconnaissance of artificial sweetener consumption and emission in Australia. Environ. Int. 143, 105963. https://doi.org/10.1016/j.envint.2020.105963

Lino, C.M., Costa, I.M., Pena, A., Ferreira, R., Cardoso, S.M., 2008. Estimated intake of the sweeteners, acesulfame-K and aspartame, from soft drinks, soft drinks based on mineral waters and nectars for a group of Portuguese teenage students. Food Addit. Contam. Part A, Chem. Anal. Control. Expo. risk Assess. 25, 1291–1296. https://doi.org/10.1080/02652030802195309

Liu, Y.Y., Blowes, D.W., Groza, L., Sabourin, M.J., Ptacek, C.J., 2014. Acesulfame-K and pharmaceuticals as co-tracers of municipal wastewater in a receiving river. Environ. Sci. Process. Impacts 16, 2789–2795. https://doi.org/10.1039/c4em00237g

Loos, R., Carvalho, R., António, D.C., Comero, S., Locoro, G., Tavazzi, S., Paracchini, B., Ghiani, M., Lettieri, T., Blaha, L., Jarosova, B., Voorspoels, S., Servaes, K., Haglund, P., Fick, J., Lindberg, R.H., Schwesig, D., Gawlik, B.M., 2013. EU-wide monitoring survey on emerging polar organic contaminants in wastewater treatment plant effluents. Water Res. 47, 6475–6487. https://doi.org/10.1016/j.watres.2013.08.024

Massmann, G., Sültenfuß, J., Dünnbier, U., Knappe, A., Taute, T., Pekdeger, A., 2008. Investigation of groundwater residence times during bank filtration in Berlin: a multi-tracer approach. Hydrol. Process. 22, 788–801. https://doi.org/https://doi.org/10.1002/hyp.6649

Massoudieh, A., 2013. Inference of long-term groundwater flow transience using environmental tracers: A theoretical approach. Water Resour. Res. 49, 8039–8052. https://doi.org/10.1002/2013WR014548

McCance, W., Jones, O.A.H., Edwards, M., Surapaneni, A., Chadalavada, S., Currell, M., 2018. Contaminants of Emerging Concern as novel groundwater tracers for delineating wastewater impacts in urban and peri-urban areas. Water Res. 146, 118–133. https://doi.org/10.1016/j.watres.2018.09.013

Molina-Giraldo, N., Bayer, P., Blum, P., Cirpka, O.A., 2011. Propagation of seasonal temperature signals into an aquifer upon bank infiltration. Ground Water 49, 491–502. https://doi.org/10.1111/j.1745-6584.2010.00745.x

Oppenheimer, J., Eaton, A., Badruzzaman, M., Haghani, A.W., Jacangelo, J.G., 2011. Occurrence and suitability of sucralose as an indicator compound of wastewater loading to surface waters in urbanized regions. Water Res. 45, 4019–4027. https://doi.org/10.1016/j.watres.2011.05.014

Ordóñez, E.Y., Quintana, J.B., Rodil, R., Cela, R., 2012. Determination of artificial sweeteners in water samples by solid-phase extraction and liquid chromatography-tandem mass spectrometry. J. Chromatogr. A 1256, 197–205. https://doi.org/10.1016/j.chroma.2012.07.073

Praveena, S.M., Cheema, M.S., Guo, H.R., 2019. Non-nutritive artificial sweeteners as an emerging contaminant in environment: A global review and risks perspectives. Ecotoxicol. Environ. Saf. 170, 699–707. https://doi.org/10.1016/j.ecoenv.2018.12.048

Purtschert, R., 2008. Natural Groundwater Quality, in: Edmunds, W.M., Shand, P. (Eds.), Natural Groundwater Quality. Blackwell Publishing, pp. 91–108. https://doi.org/10.1002/9781444300345

Renwick, A.G., 1986. The metabolism of intense sweeteners. Xenobiotica 16, 1057–1071. https://doi.org/10.3109/00498258609038983

Robertson, W.D., Van Stempvoort, D.R., Solomon, D.K., Homewood, J., Brown, S.J., Spoelstra, J., Schiff, S.L., 2013. Persistence of artificial sweeteners in a 15-year-old septic system plume. J. Hydrol. 477, 43–54. https://doi.org/10.1016/j.jhydrol.2012.10.048

Roy, J.W., Bickerton, G., 2010. Proactive screening approach for detecting groundwater contaminants along urban streams at the reach-scale. Environ. Sci. Technol. 44, 6088–6094. https://doi.org/10.1021/es101492x

Sanz-Prat, A., Greskowiak, J., Burke, V., Rivera Villarreyes, C.A., Krause, J., Monninkhoff, B., Sperlich, A., Schimmelpfennig, S., Duennbier, U., Massmann, G., 2020. A model-based analysis of the reactive transport behaviour of 37 trace organic compounds during field-scale bank filtration. Water Res. 173, 115523. https://doi.org/10.1016/j.watres.2020.115523

Scheurer, M., Brauch, H.J., Lange, F.T., 2009. Analysis and occurrence of seven artificial sweeteners in German waste water and surface water and in soil aquifer treatment (SAT). Anal. Bioanal. Chem. 394, 1585–1594. https://doi.org/10.1007/s00216-009-2881-y

Scheurer, M., Storck, F.R., Graf, C., Brauch, H.J., Ruck, W., Lev, O., Lange, F.T., 2011. Correlation of six anthropogenic markers in wastewater, surface water, bank filtrate, and soil aquifer treatment. J. Environ. Monit. 13, 966–973. https://doi.org/10.1039/c0em00701c

Sérodes, J.B., Behmel, S., Simard, S., Laflamme, O., Grondin, A., Beaulieu, C., Proulx, F., Rodriguez, M.J., 2021. Tracking domestic wastewater and road de-icing salt in a municipal drinking water reservoir: Acesulfame and chloride as co-tracers. Water Res. 203. https://doi.org/10.1016/j.watres.2021.117493

Snider, D.M., Roy, J.W., Robertson, W.D., Garda, D.I., Spoelstra, J., 2017. Concentrations of Artificial Sweeteners and Their Ratios with Nutrients in Septic System Wastewater. Groundw. Monit. Remediat. 37, 94–102. https://doi.org/10.1111/gwmr.12229

Soh, L., Connors, K.A., Brooks, B.W., Zimmerman, J., 2011. Fate of Sucralose through Environmental and Water Treatment Processes and Impact on Plant Indicator Species. Environ. Sci. Technol. 45, 1363–1369. https://doi.org/10.1021/es102719d

Spoelstra, J., Schiff, S.L., Brown, S.J., 2020. Septic systems contribute artificial sweeteners to streams through groundwater. J. Hydrol. X 7, 1–8. https://doi.org/10.1016/j.hydroa.2020.100050

Stoewer, M.M., Knöller, K., Stumpp, C., 2015. Tracing freshwater nitrate sources in pre-alpine groundwater catchments using environmental tracers. J. Hydrol. 524, 753–767. https://doi.org/10.1016/j.jhydrol.2015.03.022

Subedi, B., Kannan, K., 2014. Fate of Artificial Sweeteners in Wastewater Treatment Plants in New York State, U.S.A. Environ. Sci. Technol. 48, 13668–13674. https://doi.org/10.1021/es504769c

Theel, M., Huggenberger, P., Zosseder, K., 2020. Assessment of the heterogeneity of hydraulic properties in gravelly outwash plains: a regionally scaled sedimentological analysis in the Munich gravel plain, Germany. Hydrogeol. J. 28, 2657–2674. https://doi.org/10.1007/s10040-020-02205-y

Thiros, N.E., Gardner, W.P., Kuhlman, K.L., 2021. Utilizing Environmental Tracers to Reduce Groundwater Flow and Transport Model Parameter Uncertainties. Water Resour. Res. 57. https://doi.org/10.1029/2020WR028235

Tran, N.H., Gan, J., Nguyen, V.T., Chen, H., You, L., Duarah, A., Zhang, L., Gin, K.Y.H., 2015. Sorption and biodegradation of artificial sweeteners in activated sludge processes. Bioresour. Technol. 197, 329–338. https://doi.org/10.1016/j.biortech.2015.08.083

Tran, N.H., Nguyen, V.T., Urase, T., Ngo, H.H., 2014. Role of nitrification in the biodegradation of selected artificial sweetening agents in biological wastewater treatment process. Bioresour. Technol. 161, 40–46. https://doi.org/10.1016/j.biortech.2014.02.116

Turnadge, C., Smerdon, B.D., 2014. A review of methods for modelling environmental tracers in groundwater: Advantages of tracer concentration simulation. J. Hydrol. 519, 3674–3689. https://doi.org/10.1016/j.jhydrol.2014.10.056

Van Stempvoort, D.R., Brown, S.J., Spoelstra, J., Garda, D., Robertson, W.D., Smyth, S.A., 2020. Variable persistence of artificial sweeteners during wastewater treatment: Implications for future use as tracers. Water Res. 184, 116124. https://doi.org/10.1016/j.watres.2020.116124

Van Stempvoort, D.R., Robertson, W.D., Brown, S.J., 2011a. Artificial sweeteners in a large septic plume. Gr. Water Monit. Remediat. 31, 95–102. https://doi.org/10.1111/j.1745-6592.2011.01353.x

Van Stempvoort, D.R., Roy, J.W., Brown, S.J., Bickerton, G., 2011b. Artificial sweeteners as potential tracers in groundwater in urban environments. J. Hydrol. 401, 126–133. https://doi.org/10.1016/j.jhydrol.2011.02.013

Van Stempvoort, D.R., Roy, J.W., Grabuski, J., Brown, S.J., Bickerton, G., Sverko, E., 2013. An artificial sweetener and pharmaceutical compounds as co-tracers of urban wastewater in groundwater. Sci. Total Environ. 461–462, 348–3359. https://doi.org/10.1016/j.scitotenv.2013.05.001

Volz, M., Christ, O., Eckert, H.G., Herok, J., Kellner, H.M., Rupp, W., 1991. Kinetics and biotransformation of acesulfame-K, in: Mayer, D.G., Kemper, F.H. (Eds.), Acesulfame K. Marcel Dekker, New York, pp. 7–26.

Wolf, L., Zwiener, C., Zemann, M., 2012. Tracking artificial sweeteners and pharmaceuticals introduced into urban groundwater by leaking sewer networks. Sci. Total Environ. 430, 8–19. https://doi.org/10.1016/j.scitotenv.2012.04.059

FIGURE 1

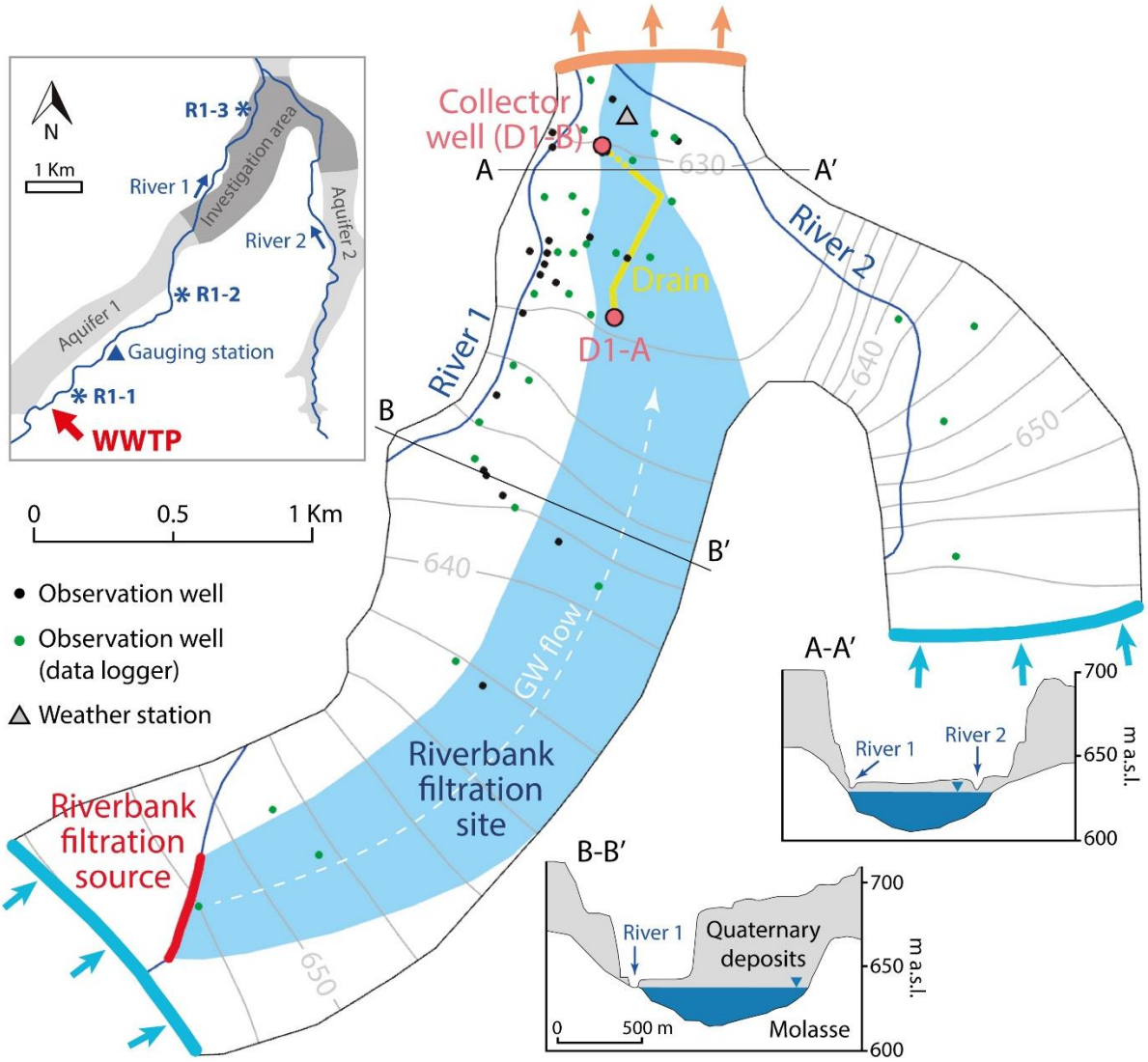

Figure 1: Hydrogeological setting of the investigation area. The top left map shows the region of the investigation area and the locations of the three water sampling points along the river (R-1, R1-2 and R1-3) and of the wastewater treatment plant (WWTP). The central map shows the riverbank filtration site, the hydraulic head contour lines (meters above sea level), the horizontal drain, groundwater sampling points D1-A and D1-B, and the main groundwater inflows (blue lines, with the blue arrows indicating the inflow direction) and outflow (orange line and arrows). The hydrogeological configuration of the aquifer is shown in the two cross-sections at the bottom right.

FIGURE 2

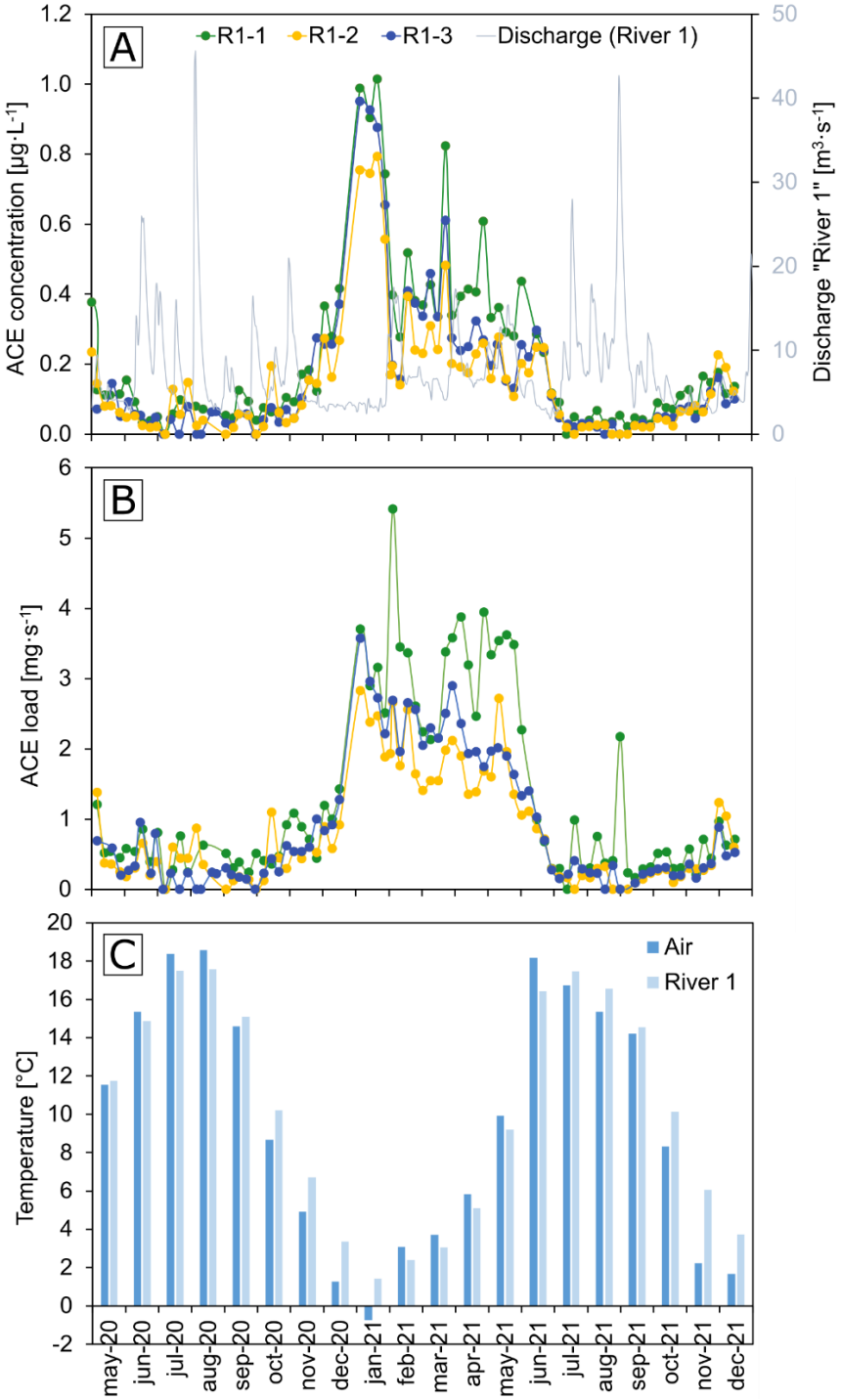

Figure 2: A) Acesulfame (ACE) concentrations in river water at sampling points R1-1, R1-2, and R1-3 (see location in Fig. 1) and river discharge. B) ACE loads for each of the three river water sampling points. C). Air and water temperature. Note the good correlation between the seasonal oscillations of temperature and the ACE load.

606 **FIGURE 3**

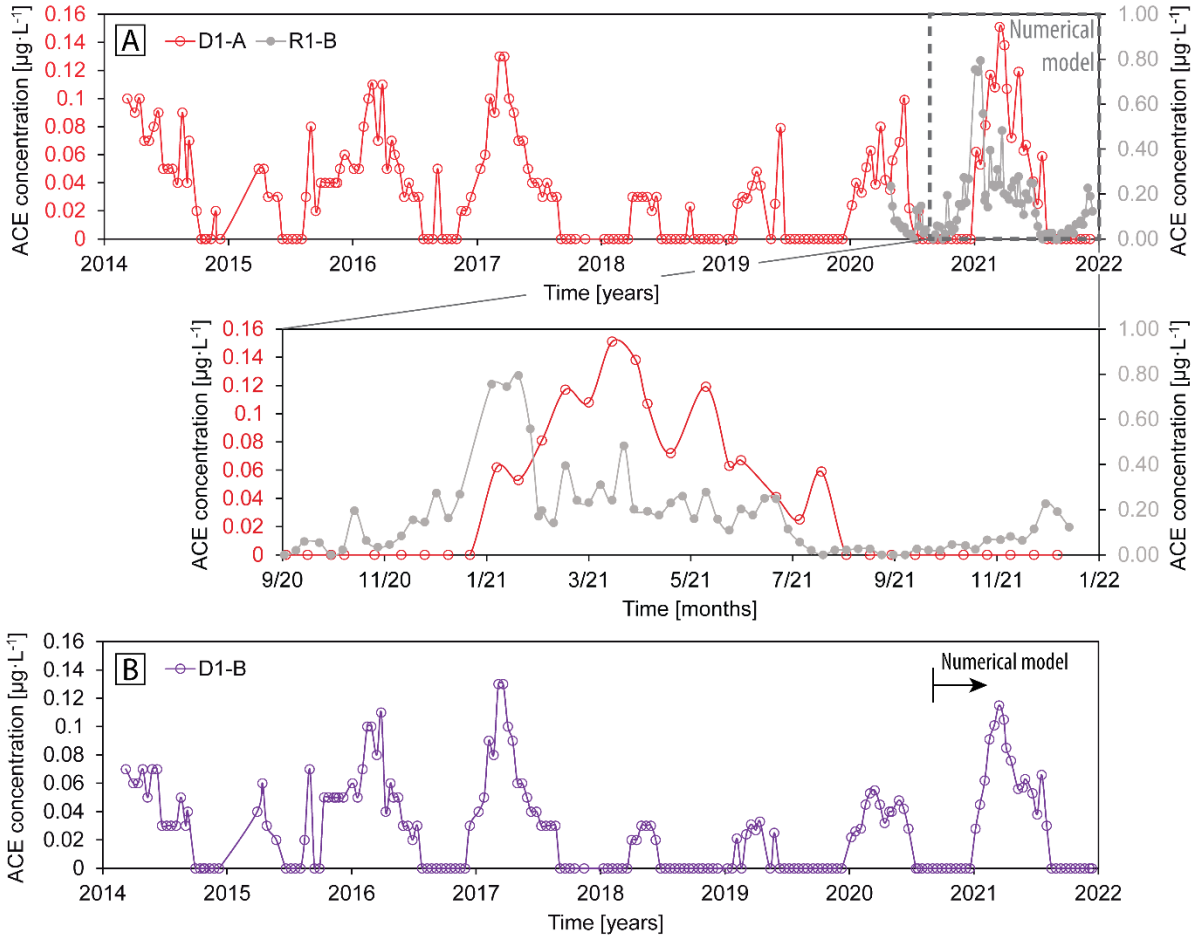

607

608 **Figure 3**: A) ACE concentrations at groundwater sampling point D1-A and its comparison with the ACE
609 concentration in river water at sampling point R1-2. A detailed view is shown for the simulated period
610 September 1, 2020 to December 31, 2021. B) ACE concentrations at groundwater sampling point D1-B.

611

612

613

614

615

616

617

618

FIGURE 4

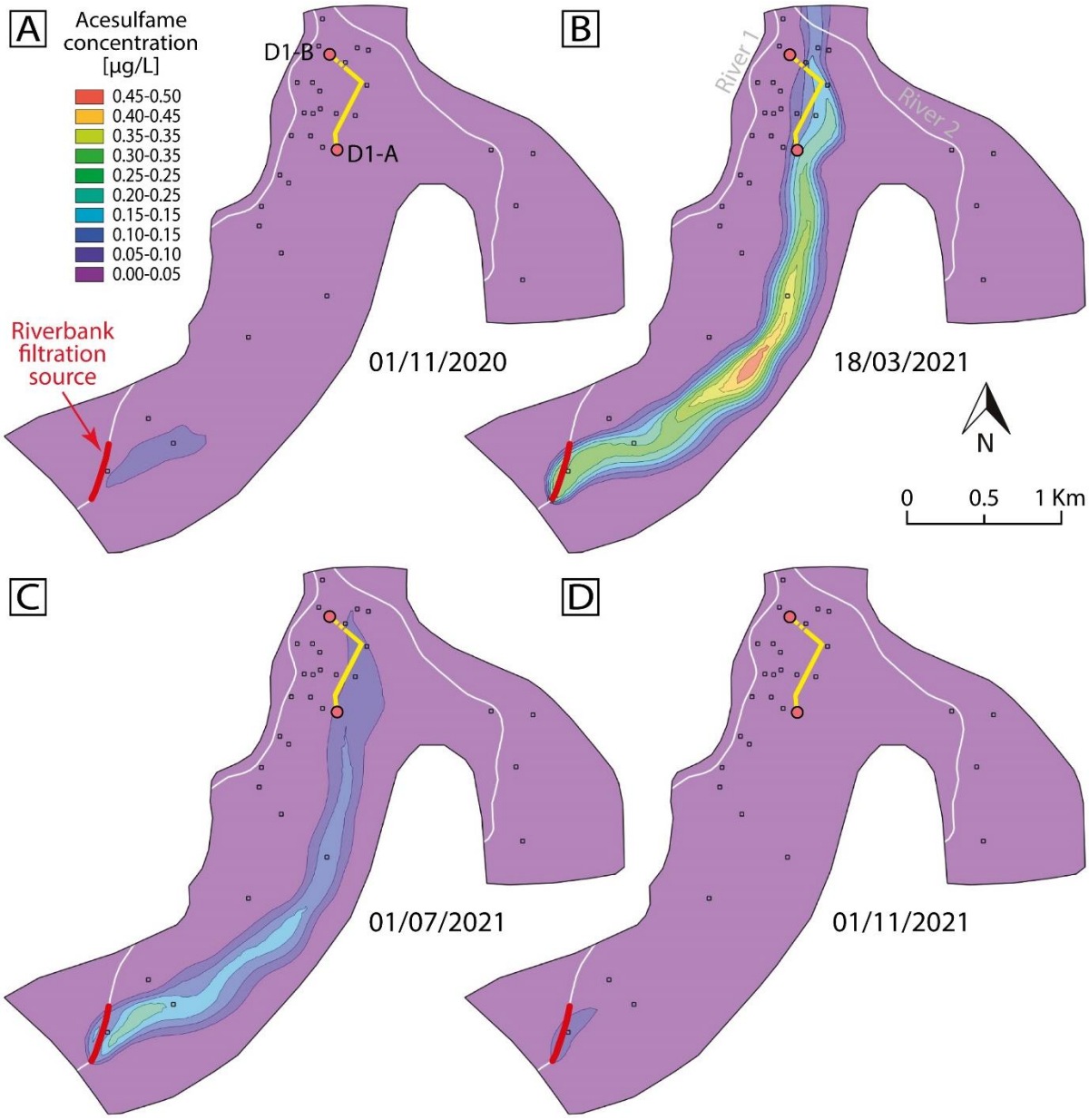

Figure 4: Simulated ACE concentrations for a complete seasonal oscillation cycle triggered by biodegradation. Note the almost negligible ACE concentrations at the end of the warm season in November (A and D) the high ACE concentrations in March (B) and at the end (C) of the cold season. Transient ACE concentrations at sampling points D1-A and D1-B are shown in Fig. 5.

FIGURE 5

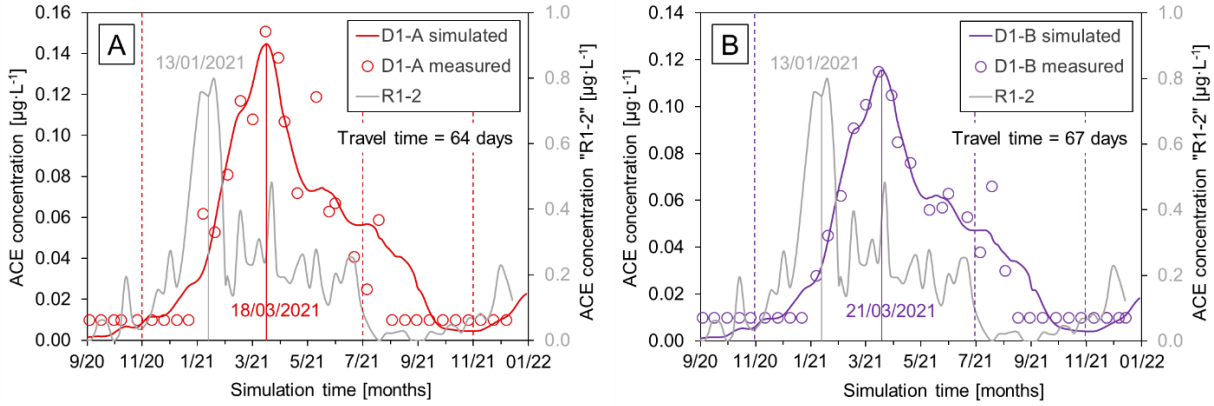

Figure 5: Simulated versus observed ACE concentrations and arrival times from the riverbank filtration source to D1-A (A) and D1-B (B) groundwater sampling points. Travel times were estimated by taking into account the concentration peaks in river water (gray line) and each of the groundwater observation points. ACE concentrations below the detection limit are plotted considering half of the LOQ (0.01 µg·L^{-1}). Dashed lines indicate the temporal location of the ACE concentration snapshots shown in Fig. 4.

650 **FIGURE 6**

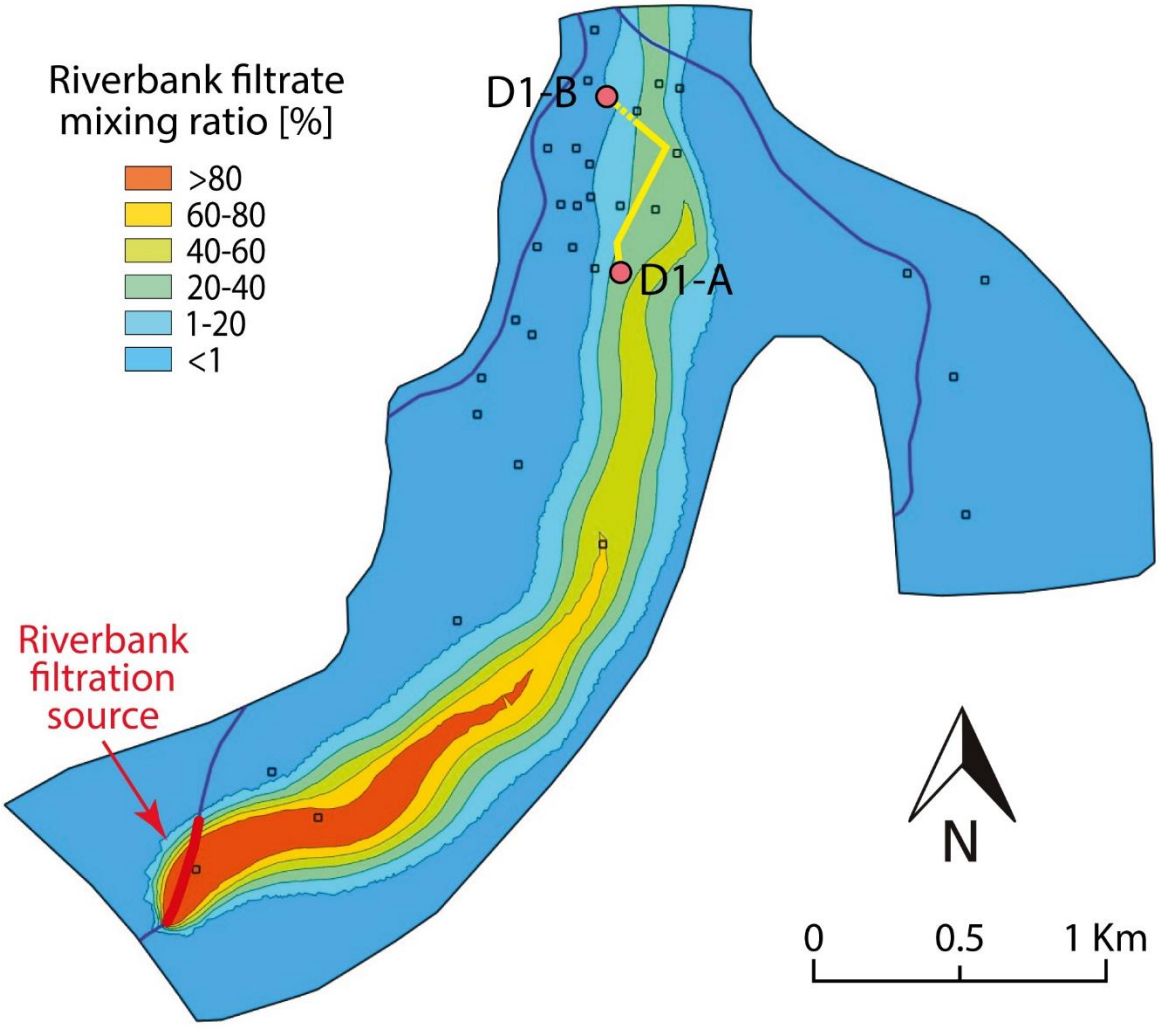

651

652 **Figure 6**: Riverbank filtration mixing ratio calculated from the model results for March 18, 2021.